Dalton
Transactions

Cite this: *Dalton Trans.*, 2012, **41**, 11898

www.rsc.org/dalton

PAPER

Temperature-/solvent-dependent low-dimensional compounds based on quinoline-2,3-dicarboxylic acid: Structures and fluorescent properties†

Ming-Fang Wang,[a] Xu-Jia Hong,[a] Qing-Guang Zhan,[a] Hong-Guang Jin,[a] Yi-Ting Liu,[a] Zhi-Peng Zheng,[a] Shi-Hai Xu[b] and Yue-Peng Cai*[a]

Received 9th June 2012, Accepted 4th August 2012
DOI: 10.1039/c2dt31243c

A series of 0-D, 1-D, and 2-D metal–organic compounds through reactions of quinoline-2,3-dicarboxylic acid (2,3-H_2qldc) with transition metal salts MCl_2, namely, M(2,3-Hqldc)$_2$(H_2O)$_2$ (M = Co(**1**), Zn(**4**) and Cd(**7**)), [M(3-qlc)$_2$(H_2O)$_2$]$_n$ (M = Co(**2**), Zn(**5**) and Cd(**8**)), M(2-qldc-3-OCH_3)$_2$(CH_3OH)$_2$ (M = Co(**3**) and Zn(**6**)) and [Cd(2,3-qldc-OCH_3)(μ_2-Cl)]$_{2n}$ (**9**) (where, 3-Hqlc = quinoline-3-carboxylic acid and 2-qldc-3-OCH_3 = 3-(methoxycarbonyl)quinoline-2-carboxylic acid), were synthesized and characterized by elemental analysis, IR, thermogravimetric analysis (TG), and single-crystal X-ray diffraction. When the temperature ranged from room temperature to 70 °C, three isomorphous mononuclear complexes **1**, **4** and **7** were obtained in H_2O/H_2O + CH_3OH. As the temperature rose further to above 90 °C, due to the decomposition of 2-position carboxyl group in ligand 2,3-H_2qldc, the same reactions, respectively, produced three isomorphous 2-D layer-like structures **2**, **5** and **8** with 4^4 topology in water. By contrast, when the mixed solvent of H_2O + CH_3OH at a 1 : 1 ratio (v/v) was applied, the three above-mentioned reactions respectively gave compounds **3**, **6** and **9** with the 3-position esterification of 2,3-H_2qldc. Compounds **3** and **6** are mononuclear and isomorphous, while complex **9** has a 1-D double-stranded chain-like structure connected by two μ_2-Cl bridges. Obviously, these results reveal that the reaction temperature and solvent play a critical role in structural direction of these low-dimensional compounds. Meanwhile, the photoluminescent property of the selected compounds is also investigated.

Introduction

Coordination polymers (CPs) or metal–organic frameworks (MOFs) involving the fields of crystal engineering and supramolecular chemistry represent a rapidly growing subject area over the last two decades, not only because of the enormous variety of interesting molecular topologies from the bridging potential of different organic linkers and geometry of the metal ions, which are often unprecedented in inorganic compounds and minerals,[1] but also due to their excellent properties with promising applications such as gas storage, gas/vapor separation, size-, shape-, and enantio-selective catalysis, luminescence and fluorescence, drug storage and delivery.[2] Due to the increasing interest in coordination polymers, an issue frequently confronted during research is whether the topology of coordination polymers and metal–organic frameworks solely based on the molecular building blocks can be predicted. And the answer at this moment is "yes, we can, to a certain extent". In fact, the proper choice of metal and organic linker ligand can already put a limit on the number of possible network architectures. Other external factors, such as type of anion, metal-to-ligand ratio, solvent, temperature, and pH also have an influence on the formation, connectivity, and topology of coordination polymers.[3] Among these influencing factors, the variation of reaction temperature and solvents, in particular, plays a very important role in the self-assembly processes of metal-complexes with different structural topologies.[4] For example, recently, Brookhart *et al.*[4a] exhibited a highly solvent- and temperature-dependent equilibrium in solution between a four coordinated Ir(I) dihydrogen species and an Ir(III) dihydride which incorporates solvent coordination on the basis of a series of NMR spectroscopic deuterium labeling studies. And Zhang *et al.*[5] also showed the effect of temperature and solvent on the morphology of microcapsules doped with a europium β-diketonate complex. In our recent work, temperature- and solvent-effects have also received much attention in the construction of metal–organic polymers.[6] Such temperature- and solvent-effects are now an important and effective route in constructing metal–organic compounds with diverse topologies and dimensionality, and so on.

---

[a] *School of Chemistry and Environment, South China Normal University; Key Laboratory of the Energy Conversion and Energy Storage Materials, Guangzhou 510006, P.R. China. E-mail: caiyp@scnu.edu.cn; Fax: +86-020-39310; Tel: +86-020-39310383*
[b] *Department of Chemistry, Jinan University, Guangzhou 510632, P.R. China. E-mail: txush@jnu.edu.cn*

† Electronic supplementary information (ESI) available. CCDC 849592, 849594, 849593, 849595, 849598, 849596, 849597, 849600 for compounds **1–6** and **8–9**, respectively. For ESI and crystallographic data in CIF or other electronic format see DOI: 10.1039/c2dt31243c

On the other hand, the N-heterocyclic dicarboxylate ligands, for example pyridine-dicarboxylic acids (H_2pydc), have attracted increasing attention in the preparation of interesting polymeric frameworks for their outstanding features of versatile coordination fashions as well as potential hydrogen-bonding donors and acceptors under hydro(solvo)thermal conditions.[7] Accordingly, pyridine-dicarboxylic acids (H_2pydc) are excellent candidates for assembling novel CPs/MOFs by incorporating appropriate metal ions in different ways, based on which many CPs/MOFs possessing beautiful and interesting topological structures are reported by our and other research groups,[8] ranging from one-dimensional (1-D) chains and two-dimensional (2-D) sheets to three-dimensional (3-D) porous structures. Of further interest, quinoline-2,3-dicarboxylic acid (2,3-H_2qldc) featuring a fused benzene ring in the 5,6-positions of the pyridine ring, as a derivative of 2,3-H_2pydc, remains largely unexplored hitherto in the field of CPs/MOFs compared with the well-studied ligands H_2pydc. 2,3-H_2pydc has a relatively large π-conjugated system in the quinoline ring, which might not only contribute much to the desirable fluorescence properties resulting from the interaction between 2,3-qldc^{2-} anions and metal ions, but also easily assemble into high dimensionality (2-D or 3-D) supramolecular networks *via* π⋯π packing interactions between two adjacent aromatic rings as well as hydrogen bonding C–H⋯π interactions, adding additional stability to these structures. Based on the above considerations, we hope to reveal some structural factors of the ligand 2,3-H_2qldc in dominating the self-assembly, which will provide more useful information of the temperature- and solvent-effects in such pyridine-based dicarboxylate ligands.

As an extension of our recent efforts to explore coordination chemistry and crystal engineering of pyridine-based dicarboxylate ligand, in this contribution, we prepared a series of low-dimensional compounds with variable topologies based on quinoline-based dicarboxylate. The syntheses, structural analysis, thermal stability, and photoluminescent properties of nine Co^{II}, Zn^{II} and Cd^{II} complexes, namely, $[M(2,3\text{-Hqldc})_2(H_2O)_2]$ (M = Co(**1**), Zn(**4**) and Cd(**7**)), $[M(3\text{-qlc})_2(H_2O)_2]_n$ (M = Co(**2**), Zn(**5**) and Cd(**8**)), $M(2\text{-qldc-3-OCH}_3)_2(CH_3OH)_2$ (M = Co(**3**) and Zn(**6**)) and $[Cd(2,3\text{-qldc-OCH}_3)(\mu_2\text{-Cl})]_{2n}$ (**9**) (where 3-Hqlc = quinoline-3-carboxylic acid, and 2-qldc-3-OCH_3 = 3-(methoxycarbonyl)quinoline-2-carboxylic acid), are presented. Our study shows that the variation of temperature and solvents in a Co^{2+}/Zn^{2+}/Cd^{2+} quinoline-2,3-dicarboxylate system can influence subtle variables that lead to coordination compounds with different structures. Especially, the temperature-driven decarboxylation and the temperature/solvent-induced esterification of the carboxyl group can control the assembly of the resulting metal–organic compounds (Scheme 1). To the best of our knowledge, this is the first example of a systematic investigation into the coordination chemistry as well as temperature- and solvent-effects in the system of quinoline-2,3-dicarboxylic acid.

Experimental

Physical measurements

All materials were reagent grade obtained from commercial sources and used without further purification, and solvents were dried by standard procedures. Elemental analyses for C, H, N were performed on a Perkin-Elmer 240C analytical instrument. IR spectra were recorded on a Nicolet FT-IR-170SX spectrophotometer in KBr pellets. Thermogravimetric analyses were performed on a Perkin-Elmer TGA7 analyzer with a heating rate of 10 °C min^{-1} in a flowing air atmosphere. The luminescent spectra for the solid state were recorded at room temperature on an Edinburgh-FLS-920 instrument with a xenon arc lamp as the light source. In the measurements of emission and excitation spectra the pass width is 5.0 nm.

Preparation of complexes 1–9

A mixture of MCl_2 (0.3 mmol) (M = Co for **1**, Zn for **4**, Cd for **7**), ligand 2,3-H_2qldc (44 mg, 0.2 mmol) and H_2O (12 mL) was heated at room temperature to 70 °C for 80 h in a 25 mL Teflon-lined stainless-steel autoclave and then cooled to room temperature at a rate of 10 °C h^{-1} to obtain the corresponding crystals.

When the temperature exceeded 90 °C, the three reactions gave three partially decarboxylated compounds **2**, **5** and **8** correspondingly. By contrast, when the mixed solvent of H_2O + CH_3OH at a 1 : 1 ratio (v/v) was used, the three above-mentioned reactions gave the partially esterified compounds **3**, **6** and **9**, respectively.

1. Yield 65% (based on the Co), yellow crystals. Elemental analysis calcd (%) for $C_{22}H_{16}N_2O_{10}Co$: C,50.07; H,3.06; N,5.34. Found: C,50.10; H,3.08; N,5.31. FT-IR (KBr, cm^{-1}): 3367(br,vs), 1728(vs) 1678(vs), 1554(vs), 1458(vs), 1373(s), 1273(w), 1184(m), 1157(m), 910(m), 856(m), 775(m), 748(w), 682(w), 536(w), 459(w).

2. Yield 49% (based on the Co), yellow crystals. Elemental analysis calcd (%) for $C_{20}H_{12}N_2O_4Co$: C,59.52; H,2.98; N,6.94. Found: C,55.48; H,2.97; N,7.01. FT-IR (KBr, cm^{-1}): 3413(br, w), 1633(vs), 1595(m), 1463(vs) 1382(vs), 1282(s), 1209(s), 1152(s), 938(m), 897(w), 789(m), 747(m), 664(m), 600(m), 566(m), 488(w).

3. Yield 48% (based on the Co), yellow crystals. Elemental analysis calcd (%) for $C_{26}H_{24}N_2O_{10}Co$: C,53.48; H,4.11; N,4.8. Found: C,53.55; H,4.13; N,4.68. FT-IR (KBr, cm^{-1}): 3228(br, w), 1643(vs), 1558(m), 1458(s), 1377(m), 1249(s), 1176(w), 1138(w), 906(w), 856(m), 798(m), 783(m), 667(w), 621(w), 493(w), 455(w).

4. Yield 51% (based on the Zn), colorless crystals. Elemental analysis calcd (%) for $C_{22}H_{16}N_2O_{10}Zn$: C,50.07; H,2.71; N,4.75. Found: C,50.17; H,2.80; N,4.70. FT-IR (KBr, cm^{-1}): 3367(br,vs), 1728(vs) 1678(vs), 1554(vs), 1458(vs), 1373(s), 1273(w), 1184(m), 1157(m), 910(m), 856(m), 775(m), 748(w), 682(w), 536(w), 459(w).

5. Yield 71% (based on the Zn), colorless crystals. Elemental analysis calcd (%) for $C_{20}H_{12}N_2O_4Zn$: C,58.58; H,2.93; N,6.83. Found: C,58.47; H,2.99; N,6.73. FT-IR (KBr, cm^{-1}): 3413(br, w), 1633(vs), 1595(m), 1463(vs), 1382(vs), 1282(s), 1209(s), 1152(s), 938(m), 897(w), 789(m), 747(m), 664(m), 600(m), 566(m), 488(w).

6. Yield 50% (based on the Zn), colorless crystals. Elemental analysis calcd (%) for $C_{26}H_{24}N_2O_{10}Zn$: C,50.07; H,2.71; N,4.75. Found: C,50.17; H,2.80; N,4.70. FT-IR (KBr, cm^{-1}): 3228(br,w), 1643(vs), 1558(m), 1458(s), 1377(m), 1249(s),

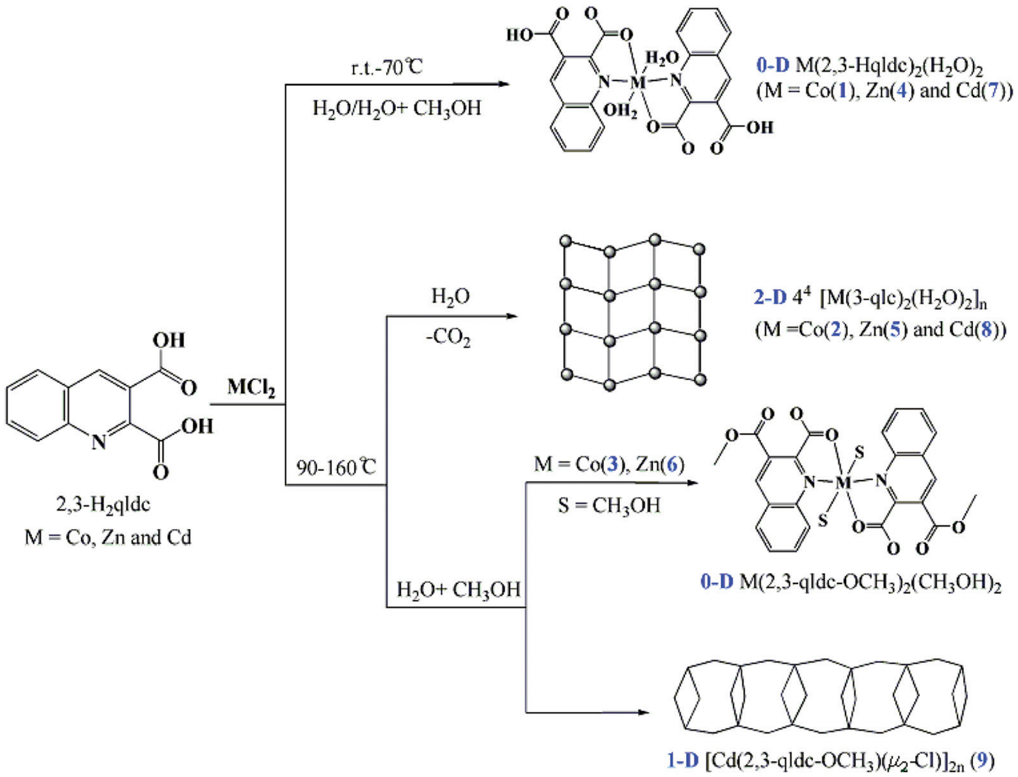

Scheme 1 Assembly of compounds **1–9** controlled by temperature and solvents.

1176(w), 1138(w), 906(w), 856(m), 798(m), 783(m), 667(w), 621(w), 493(w), 455(w).

7. Yield 67% (based on the Cd), colorless crystals. Elemental analysis calcd (%) for $C_{22}H_{16}N_2O_{10}Cd$: C,50.07; H,3.06; N,5.34. Found: C,55.17; H,3.08; N,5.31. FT-IR (KBr, cm^{-1}): 3367(br,vs), 1725(w), 1678(vs), 1554(vs), 1458(vs), 1373(s), 1273(w), 1184(m), 1157(m), 910(m), 856(m), 775(m), 748(w), 682(w), 536(w), 459(w).

8. Yield 66% (based on the Cd), colorless crystals. Elemental analysis calcd (%) for $C_{20}H_{12}N_2O_4Cd$: C,52.55; H,2.63; N,6.13. Found: C,52.47; H,2.68; N,6.11. FT-IR (KBr, cm^{-1}): 3413(br, w), 1633(vs), 1595(m), 1463(vs), 1382(vs), 1282(s), 1209(s), 1152(s), 938(m), 897(w), 789(m), 747(m), 664(m), 600(m), 566(m), 488(w).

9. Yield 49% (based on the Cd), colorless crystals. Elemental analysis calcd (%) for $C_{12}H_8NClO_4Cd$: C,38.10; H,2.12; N,3.70. Found: C,38.17; H,2.18; N,3.64. FT-IR (KBr, cm^{-1}): 3363(br, w), 1643(vs), 1546(m), 1454(vs), 1384(s), 1346(s), 1207(m), 1141(s), 1056(m), 906(w), 852(m), 817(m), 775(m), 748(m), 671(m), 594(m), 543(w), 474(w).

X-ray data collection and structure refinement

Data collections were performed at 298 K on a Bruker Smart Apex II diffractometer with graphite-monochromated MoKα radiation (λ = 0.71073 Å) for **1–6**, and **8–9**. Absorption corrections were applied by using the multiscan program SADABS.[9] Structural solutions and full-matrix least-squares refinements based on F^2 were performed with the SHELXS-97[10] and SHELXL-97[11] program packages, respectively. All the non-hydrogen atoms were refined anisotropically. The hydrogen atoms were placed at calculated positions and included in the refinement in the riding model approximation. The organic hydrogen atoms were generated geometrically (C–H = 0.93 or 0.96 Å), and the water hydrogen atoms were located from difference maps and refined with isotropic temperature factors. Details of the crystal parameters, data collections, and refinements for complexes **1–6** and **8–9** are summarized in Table S1.† Selected bond lengths and angles for eight complexes are shown in Table S2,† hydrogen-bonding data of these eight complexes are listed in Table S3 (ESI†). Further details are provided in the ESI.† Crystallographic data for the structures reported in this paper have been deposited with the Cambridge Crystallographic Data Centre.

Results and discussion

Synthetic and spectral aspects

Through conventional solution reaction or hydro(solvo)thermal syntheses, nine new compounds **1–9** were synthesized and characterized by EA, IR and X-ray single-crystal diffraction. Although compound **7** has no single crystal structure, the results of its EA and TG confirm that **7** and **1**, **4** are isomorphous. When the reaction medium is water, the major ligand 2,3-H_2qldc reacting with $M^{II}Cl_2$ easily lost one 2-position carboxyl group under high temperature (for **2**, **5** and **8**). However, when the mixture solvent of H_2O + CH_3OH is used, due to partial esterification of ligand 2,3-H_2qldc at high temperature, three compounds **3**, **6** and **9** were obtained, indicating temperature and solvent have a certain effect on the formation of these metal–organic compounds in the 2,3-H_2qldc system.

The IR spectra of **1–9** are similar. The strong and broad absorption bands in the range of 3100–3600 cm^{-1} of these compounds may be assigned to the characteristic peaks of ν_{O-H} stretching vibrations from coordinated water or methanol molecules. The strong vibrations appearing around 1635, 1590, and 1450 cm^{-1} correspond to the asymmetric and symmetric stretching vibrations of the carboxyl group, respectively.[12] The absence of strong bands ranging from 1690 to 1730 cm^{-1} for complexes **2**, **3**, **5**, **6**, **8** and **9** indicates that the ligand in these complexes are deprotonated, compared with those of free ligands in these complexes.

Thermal stability of the complexes was investigated by the TGA technique (see Fig. S1, ESI†). The isomorphous phenomenon exists in nine compounds **1–9**, so only four compounds **1**, **2**, **3** and **9** were selected to examine their thermal stability. The TGA curve of compound **1** shows that the weight loss of 7.10% around 115 °C attributes to the removal of coordinated water (calc. 6.83%). Then the framework remains integrity until 261 °C (Fig. S1a†). The TGA curve of **2** shows the complex is very steady and there is no weight loss until 293 °C (Fig. S1b†). The TGA curve of **3** shows continuous weight losses in the temperature range of 122–167 °C are because of the removal of coordinated methanol molecules. The observed weight loss of 10.15% is in good agreement with the calculated value (10.97%). Then the framework begins to decompose when the temperature rise up to 226 °C (Fig. S1c†). The TGA curve of compound **9** shows the complex begins to lose weight up to 270 °C and then begins to decompose (Fig. S1d†).

Structural analysis and discussion

M(2,3-Hqldc)$_2$-(H_2O)$_2$ (M = Co(1) and Zn(4)). The 0-D mononuclear coordination compounds **1** and **4** are isostructural and crystallize in the triclinic space group $P\bar{1}$. Here, we choose **1** to represent the detailed structure. The mononuclear molecule contains one Co^{II} cation, two partially deprotonated 2,3-$Hqldc^-$ anions and two coordinated water molecules. The coordination number of Co1 is six with two nitrogen and four oxygen atoms from two individual ligands 2,3-$qldc^-$ and two coordinated water molecules. The coordination geometry of the Co(II) center is a slightly distorted octahedron as shown in Fig. 1. The Co–O distances are in the range of 2.027(3)–2.093(3) Å and the Co–N distance is 2.228(4) Å. Only one of the two carboxyl groups in ligand 2,3-H_2qldc was deprotonated and adopts the μ-η^1:η^1 coordination fashion (mode **I** in Scheme 2). In addition to intramolecular hydrogen bonds O(C)–H···O, the intermolecular hydrogen bond O–H···O also plays an important role in assembling the mononuclear molecule Co(2,3-Hqldc)$_2$(H_2O)$_2$ into 2-D supramolecular network (Fig. 2). From Fig. 2a, each neutral mononuclear unit forms a series of acceptor/donor hydrogen bonds with four neighbouring ones *via* intermolecular hydrogen bonds involving O–H···O, leading to the formation of a two-dimensional ordered layer-like structure. If the mononuclear unit is viewed as the node and the hydrogen bonding O–H···O interaction from four neighbouring ones as linkers (Fig. 2b), the resulted 2D supramolecular structure may be simplified into a two-dimensional 4^4 rhombic-grid as depicted in Fig. 2b.

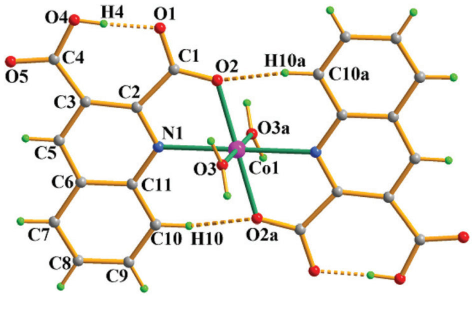

Fig. 1 The coordination environments of the Co^{II} ion in compound **1** containing intramolecular hydrogen bonds O(C)–H···O. Symmetry code: (a) $1 - x$, $-y$, $1 - z$.

[M^{II}(3-qlc)$_2$(H_2O)$_2$]$_n$ (M = Co(2), Zn(5) and Cd(8)). When heated up to 90–160 °C, the reactions of 2,3-H_2qldc with MCl_2 gave three isostructural complexes **2** (M = Co), **5** (M = Zn) and **8** (M = Cd). Considering the isomorphous phenomenon, only the structure of complex **2** is described in detail. Single crystal X-ray diffraction shows that complex **2** crystallized in the monoclinic space group *C*2/*c*, in which the ligand 2,3-H_2qldc became 3-qlc^- *via* 2-position decarboxylation. As shown in Fig. 3, the Co1 is five coordinated to three O atoms from two 3-qlc^- and two N atoms from two other 3-qlc^-, and exhibits the coordination geometry of a distorted square-pyramid around the cobalt(II) ion with the N2 atom occupying the apical position and O1, N1, O2, O3 defining the basal plane. The Co–O distances are 1.936(2) and 1.977(2) Å and the Co–N distances are 2.085(2) and 2.103(2) Å. Every ligand 3-qdc^- in **2**, in which ligand 3-qdc^- adopts two coordination manners, namely mode **II**: μ_2-η^1:η^1 and mode **III**: μ_2-η^1:η^1:η^1 in Scheme 2, links two Co^{2+} ions using one/two O atoms from carboxyl and one N atom to form a 2D layer-like structure (Fig. 4a). When we consider the Co^{II} as the node and the ligand as the linker, the simplified topological representation of compound **2** can be described in Fig. 4b, which exhibits a 4-connected 4^4 topology with one wave side.

Moreover, inter-layer π···π stacking interaction with the distance of 3.761 Å between the centers of two benzene/pyridine rings, links the adjacent coordination layers to form a 3-D network (Fig. 5).

M(2,3-qldc-OCH_3)$_2$(CH_3OH)$_2$ (M = Co(3) and Zn(6)). As the control, when the mixed solvent of $H_2O + CH_3OH$ at a 1 : 1 ratio (v/v) was applied, the reaction of 2,3-H_2qldc with MCl_2 gave three compounds **3**, **6** and **9** with the 3-position esterification of 2,3-H_2qldc. Single crystal X-ray diffraction shows that two complexes **3** and **6** are isostructural and crystallize in the monoclinic space group *P*2(1)/*c*. Similarly, compound **3** is selected to represent the two structures. In **3**, as shown in Fig. 6, the mononuclear molecule contains one Co^{II} centers, two esterified 2,3-(qldc-OCH_3)$^-$ units and two coordinated methanol molecules. The Co1 is six-coordinated by two nitrogen and four oxygen atoms from two esterified individual ligands 2,3-(qldc-OCH_3)$^-$ and two coordinated methanol molecules. The Co–O distances are in the range of 2.008(3)–2.125(4) Å and the Co–N distance is 2.218(4) Å. Because one of the two carboxyl groups in ligand

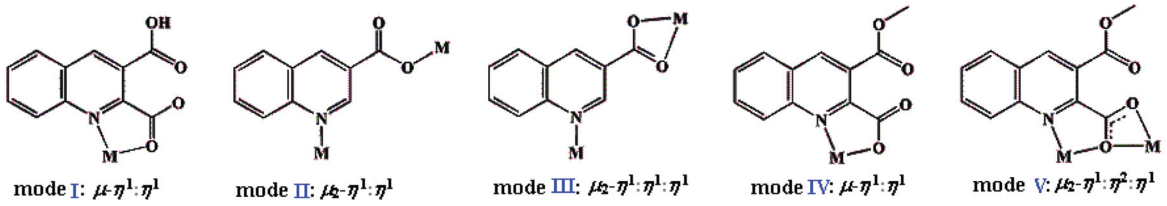

Scheme 2 Coordination modes of 2,3-qldc^{2-}, as well as 2,3-(qldc-OCH$_3$)$^-$ and 3-qlc$^-$ after partial esterification and decarboxylation in **1–9**.

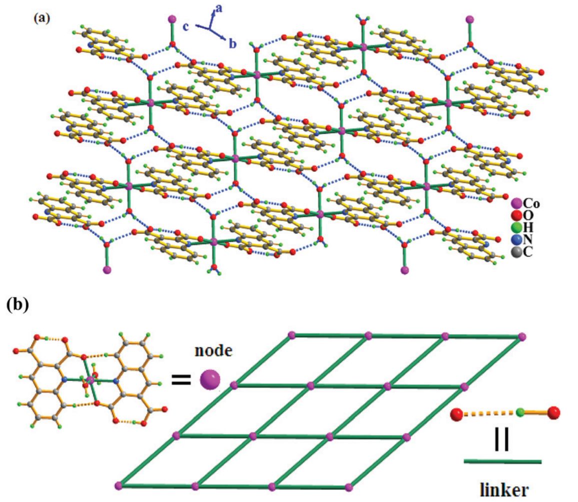

Fig. 2 (a) 2-D supramolecular layer constructed by neutral mononuclear unit Co(2,3-Hqldc)$_2$(H$_2$O)$_2$ *via* the intermolecular hydrogen bond O–H···O. (b) Two-dimensional 4^4 rhombic-grid in compound **1**.

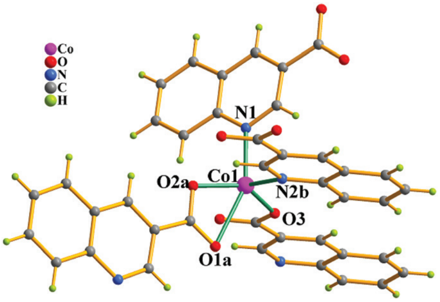

Fig. 3 The coordination environments of the Co^{II} ion in compound **2** containing partial atomic labels. Symmetry code: (a) x, $1 - y$, $0.5 + z$; (b) x, $-1 + y$, z.

2,3-H$_2$qldc was esterified, the new ligand 2,3-qldc-OCH$_3$ adopts the μ-η^1:η^1 coordination fashion (mode **IV** in Scheme 2). Similar to compound **1**, in addition to an intramolecular hydrogen bond C–H···O, each neutral mononuclear molecule Co(2,3-qldc-OCH$_3$)$_2$(CH$_3$OH)$_2$ interacts with four neighbouring ones *via* intermolecular hydrogen bonding involving O3–H3···O2 (Table S2†) leading to the formation of a 2-D 4^4 supramolecular network, in which the mononuclear unit is viewed as the node and the hydrogen bonding O–H···O interaction from four neighbouring ones as linkers (Fig. 7).

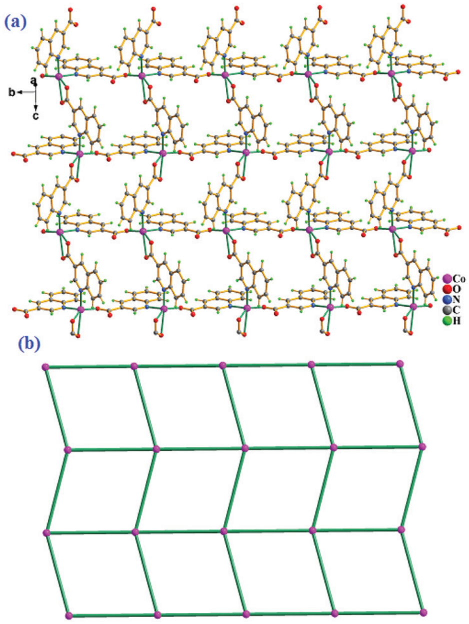

Fig. 4 2-D wave-like sheet with 4^4 topology extended in *bc* plane in **2**.

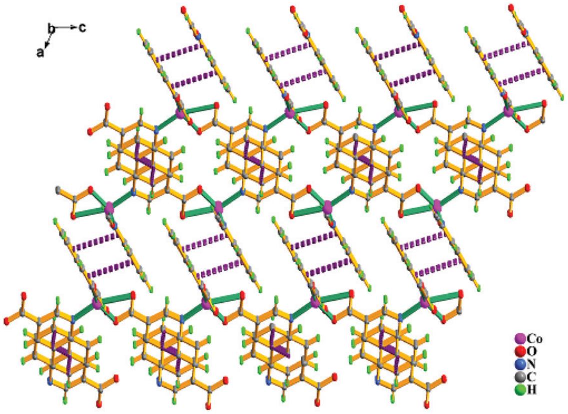

Fig. 5 3-D supramolecular network constructed by inter-layer π···π interaction along *b* axis in **2**.

[Cd(2,3-qldc-OCH$_3$)(μ$_2$-Cl)]$_{2n}$ (9). When warming to above 90 °C, in the mixed solvent of H$_2$O + CH$_3$OH, the reaction of 2,3-H$_2$qldc with CdCl$_2$ gave a 1-D chain-like complex **9**, which is different from the above-discussed mononuclear complexes **3** and **6**. Single crystal X-ray diffraction shows that complex **9** crystallized in the monoclinic space group *C*2/*c*. The asymmetric unit contains one crystallographically independent Cd(II) ion,

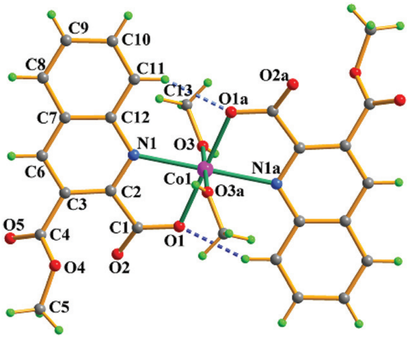

Fig. 6 The coordination environments of the Co^{II} ion in compound **3** containing partial atomic labels. Symmetry code: (a) $1 - x$, $1 - y$, $1 - z$.

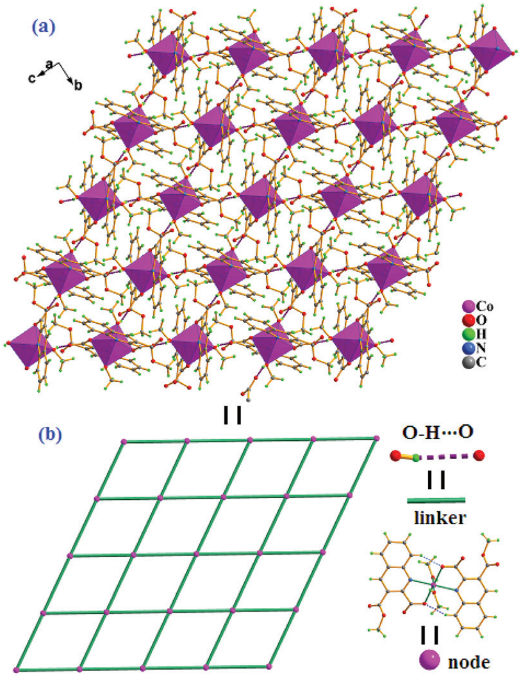

Fig. 7 2-D supramolecular layer with 4^4 topology constructed by intermolecular hydrogen bond O–H···O extended in the *bc* plane in **3**.

one esterified 2,3-$(qldc\text{-}OCH_3)^-$ unit, and one μ_2-Cl^- anion (Fig. 8). Cd^{2+} ion in compound **9** is six-coordinated by one nitrogen and three oxygen atoms from two individual ligands as well as two μ_2-Cl atoms, and shows octahedral coordination geometry with O4 and O4a atoms at axial positions and the four remaining positions are occupied by N1, O3a and two μ_2-bridging Cl1, Cl1b in a square plane. The Cd–O distance is in the range of 2.300(11)–2.472(11) Å and the Cd–N distance 2.395(8) Å. In this structure, the partially esterified 2,3-$(qldc\text{-}OCH_3)^-$ exhibits the coordination mode **V**: μ_2-η^1:η^2 as shown in Scheme 2. The coordinated O4 atom in ligand 2,3-$(qldc\text{-}OCH_3)^-$ adopts a μ_2-mode to bridge two Cd to form a 1-D $(\text{–O–Cd–O–})_n$ chain, and then through two μ_2-Cl bridges, the two adjacent $(\text{–O–Cd–O–})_n$ chains are connected to form a 1-D ladder-like chain structure (Fig. 9). These 1-D chains are further assembled into 3-D supermolecular layer through inter-layer π···π stacking interactions between the adjacent quinoline rings (Fig. 10).

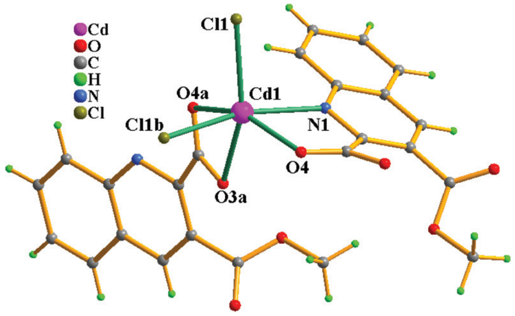

Fig. 8 Perspective views of the coordination environments of the Cd^{II} ions in compound **9**. Symmetry code: (a) x, $-y$, $-0.5 + z$; (b) $-x$, $-y$, $1 - z$.

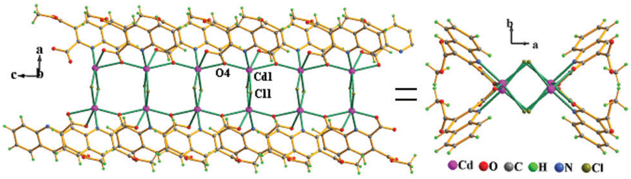

Fig. 9 1-D double-stranded chain connected by two μ_2-Cl bridges in compound **9**.

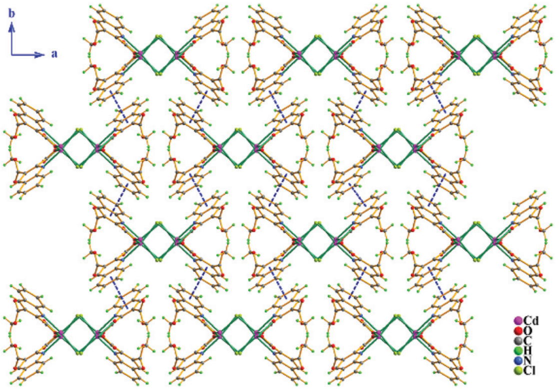

Fig. 10 3-D supramolecular network constructed by intra-chain π···π stacking interactions along the *c* axis in **9**.

Effect of temperature and solvent on molecular assemblies. In this article crystal structures of the Co(II)/ Zn(II)/Cd(II)/quinoline-2,3-dicarboxylate system have been described and discussed, which have been prepared with either a single-medium of H_2O or a mixed-medium of H_2O + CH_3OH in the range of room temperature to 160 °C. From the above description and discussion, it can be seen that different reaction temperatures/solvents have a great influence on the assembly of these metal–organic complexes. The overview presented in Scheme 1 shows that *via* the hydro-/solvothermal synthesis method in a solvent of H_2O/ H_2O + CH_3OH, 0-D mononuclear compounds (**1**, **4** and **7**) were always obtained with an integrity of ligand 2,3-H_2qldc in the range of r.t to 70 °C, indicating the solvent seemed to have no influence on the topology of the final compounds in the present reaction system at low temperature. With the rise of temperature from 90 to 160 °C, the reaction between 2,3-H_2qldc and MCl_2 in

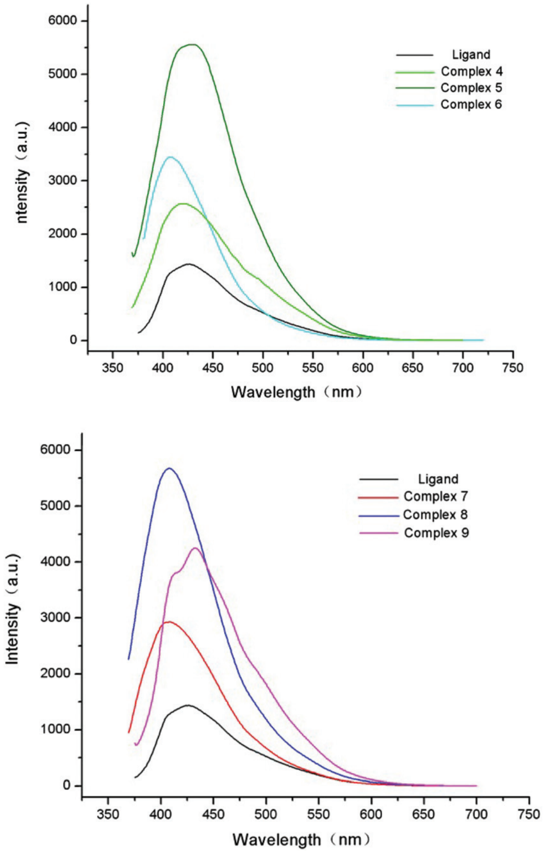

Fig. 11 Luminescent behaviors of compounds **4–9** in the solid state at room temperature.

H_2O gave 2-D 4^4 isostructural compounds **2**, **5** and **8** with the decarboxylation of 2-position carboxyl group in 2,3-H_2qldc, which suggests that the temperature plays an important role in the present case. While the reaction solvent is changed from H_2O to H_2O + CH_3OH, the topology of the resultant complexes is altered from 2-D partially decarboxylated compounds **2**, **8** and **11** to 0-D/1-D partially esterified compounds **3**, **6** and **9**, showing the solvent also has an influence on the topology of the final products.

Further analysis found that in the present study, the different coordination modes of these ligands of 2,3-H_2qldc, as well as its derivatives of 2,3-Hqldc-OCH_3 and 3-Hqldc are the underlying reason behind the differences in the structure of this series of M^{II} complexes. At low temperature, the ligand 2,3-H_2qldc mainly adopted a simple fashion **I** with an NO chelating coordination mode to give 0-D mononuclear compounds, and uncoordinated 3-position carboxylic group easily forms intermolecular hydrogen bonds, resulting in the formation of more stable supramolecular structures (for example, **1** and **4**). At high temperature, the ligand 2,3-H_2qldc reacting with MCl_2 in the medium of H_2O easily decarboxylated at the 2-position to give μ_2-bridging ligand 3-$qldc^-$ in favor of the assembly of 2-D metal–organic complexes (for instance, **2**, **5** and **8**). Meanwhile, because of the existence of the big aromatic quinoline ring in the ligand 2,3-H_2qldc, the 3-D order supramolecular structure is also easily assembled through inter-layer π···π stacking interactions.

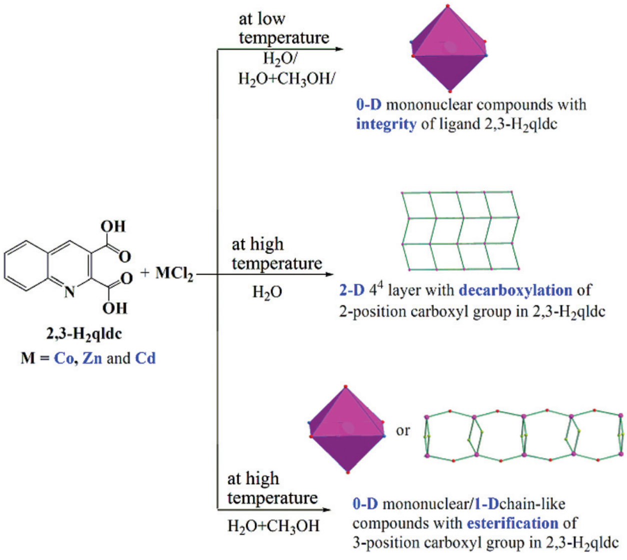

Scheme 3

However, when the mixed solvent of H_2O + CH_3OH served as the reaction medium, after the N atom and the O atom from the 2-position carboxylic group of 2,3-H_2qldc coordinated to the central metal in a chelating fashion, the 3-position carboxylic group is susceptible to esterification by methanol at high temperature. Compared to the carboxylic group, the coordination ability of the ester to the metal ion is weaker. Hence coordination sites of ligand 2,3-$(qldc\text{-}OCH_3)^-$ were reduced after esterification, making it very easy to understand the formation of the resultant mononuclear compounds such as **3** and **6**. It is noteworthy that, in present reaction system, compound **9** is a 1-D double-stranded chain rather than a 0-D mononuclear compound. An explanation for this observation has not yet been found, but it certainly has to do with the cation, since this is the only difference among the three compounds **3**, **6** and **9**. Cd^{2+} ion has the largest ionic radius among the three ions involved Co^{2+}(**3**), Zn^{2+}(**6**) and Cd^{2+}(**9**), which makes it possible for the counter-anion Cl^- to further coordinate to Cd^{2+} ion in a μ_2-bridging fashion, resulting in the formation of the 1-D chain in compound **9**. As indicated above, obviously directing coordination of these quinoline-involved ligands to metal centers is the synergy of various factors, but the temperature and solvent indeed play an important role in inducing the arrangement and coordination modes of the ligands, subsequently leading to different topological structures of metal–organic complexes in the present reaction system and under the reaction conditions employed (Scheme 3).

Luminescent property

As reported previously, metal–organic compounds have the ability to affect the emission wavelength and intensity of the organic material through metal coordination.[13] Therefore, it is important to investigate the luminescent properties of metal–organic compounds in view of their potential applications. The luminescent behaviors of compounds **4–9** and free ligands were investigated in the solid state at room temperature as shown in Fig. 11. Apparently, the emission spectra of the complexes resemble that of free ligands except for the emission intensity and peak positions, indicating that the fluorescence of the complexes are ligand-based emission. Meanwhile, green emission for the complexes and ligands is observed, where the maximum emission wavelength is 428 nm (under 361 nm excitation) for the free ligands 2,3-H_2qldc, 408, 428 and 421 for complexes **4**, **5**, **6** (corresponding excitation under 359, 355 and 359 nm), and 408, 408 and 432 for complexes **7**, **8**, **9** (corresponding excitation under 359, 355 and 359 nm), respectively. Compared with the emission spectra of 2,3-H_2qldc, a varying degree of blue shifts of 20 nm in **4**, **7** and **8**, 7 nm in **6** and red shifts of 4 nm in **9** were observed, which are derived from the different topological, supramolecular structures and different dimensions. Moreover, from Fig. 11, we find that the fluorescent intensity of complexes **5** and **8** are stronger than that of others, and it may be attributed to complexes **5** and **8** possessing a 2-D framework structure while the others have a 0D or 1D structure. As for **9** with a stronger peak than **7**, there is a possible explanation that **9** has a 1-D chain-like structure and can be assembled into a 3-D supramolecular network by intra-chain stacking interactions. Meanwhile, the enhanced fluorescence intensities of these complexes are detected, which indicates that it is a good candidate material for photochemical applications of these complexes, especially for complexes **5** and **8**.[13]

Conclusions

In summary, a series of low-dimensional transition metal complexes with dimensional diversity based on 2,3-H_2qldc have been successfully synthesized in different solvents and under different temperatures for the first time. At low temperature, the reaction of 2,3-H_2qldc with MCl_2 always gave 0-D mononuclear compounds (**1**, **4** and **7**) with integrity of ligand 2,3-H_2qldc. At high temperature, the same reaction in H_2O offered 2-D 4^4 isostructural compounds **2**, **5** and **8** with decarboxylation of the 2-position carboxyl group in 2,3-H_2qldc, however, changing the reaction solvent from H_2O to $H_2O + CH_3OH$, the topology of the resultant complexes was altered from 2-D partially decarboxylated compounds **2**, **5** and **8** to 0-D/1-D partially esterified compounds **3**, **6** and **9**. Based on which *via* different intermolecular weaker interactions such as hydrogen bonding O(C)–H⋯O and π⋯π packing interactions, different dimensionality and topological supramolecular networks were assembled. Obviously, in the present reaction system, the selection of temperature and solvent is critical in determining the molecular and supramolecular structures of the resultant complexes **1–9**. Further investigation revealed that the different coordination modes of these ligands of 2,3-H_2qldc, as well as its derivatives of 2,3-Hqldc-OCH_3 and 3-Hqldc are the underlying reason behind the differences in the structure of this series of M^{II} complexes. More importantly, changes in structure are accompanied by changes in fluorescent properties due to different molecular aggregations and, thus, different crystal structures. The relationship between structures and properties may provide a useful strategy to tune the fluorescent properties of metal–organic compounds, which could be exploited as building blocks for nano-scale optoelectronic devices. In fact, for a rational design and understanding of new coordination polymer systems, one should first systematically analyze the effect of the related parameters in order to filter out those ones that really determine the desired network properties.

Acknowledgements

The authors are grateful for financial aid from the National Natural Science Foundation of P. R. China (Grant Nos. 91122008 and 21071056), Science and Technology Planning Project of Guangdong Province (Grant No. 2010B031100018) and the N. S. F. of Guangdong Province (Grant No. 9251063101000006) and Science and information Technology of Guangzhou Municipal (Grant No. 2011J52090019).

References

1 (*a*) O. M. Yaghi, M. O'Keeffe, N. W. Ockwig, H. K. Chae, M. Eddaoudi and J. K. Reticular, *Nature*, 2003, **423**, 705; (*b*) S. Kitagawa, R. Kitaura and S. Noro, *Angew. Chem., Int. Ed.*, 2004, **43**, 2334; (*c*) F. Blank and C. Janiak, *Coord. Chem. Rev.*, 2009, **253**, 827; (*d*) X.-H. Bu, W. Chen, W.-F. Hou, M. Du, R.-H. Zhang and F. Brisse, *Inorg. Chem.*, 2002, **41**, 3477; (*e*) X.-H. Bu, Y.-B. Xie, J.-R. Li and R.-H. Zhang, *Inorg. Chem.*, 2003, **42**, 7422; (*f*) X.-H. Bu, M.-L. Tong, Y.-B. Xie, J.-R. Li, H.-C. Chang, S. Kitagawa and J. Ribas, *Inorg. Chem.*, 2005, **44**, 9837.

2 (*a*) O. Shekhah, H. Wang, M. Paradinas, C. Ocal, B. Schüpbach, A. Terfort, D. Zacher, R. A. Fischer and C. Wöll, *Nat. Mater.*, 2009, **8**, 481; (*b*) S. K. Henninger, H. A. Habib and C. Janiak, *J. Am. Chem. Soc.*, 2009, **131**, 2776; (c) T. Yamada and H. Kitagawa, *J. Am. Chem. Soc.*, 2009, **131**, 3144; (*d*) B. Gil-Hernández, P. Gili, J. K. Vieth, C. Janiak and J. Sanchiz, *Inorg. Chem.*, 2010, **49**, 7478.

3 (*a*) F. Hung-Low, A. Renz and K. K. Klausmeyer, *Polyhedron*, 2009, **28**, 407; (*b*) S. K. Ghosh and S. Kitagawa, *CrystEngComm*, 2008, **10**, 1739; (*c*) X.-M. Lin, H.-C. Fang, Z.-Y. Zhou, L. Chen, J.-W. Zhao, S.-Z. Zhu and Y.-P. Cai, *CrystEngComm*, 2009, **11**, 847; (*d*) L. Pan, X. Huang and X. Li, *J. Solid State Chem.*, 2000, **152**, 236; (*e*) L. Pan, T. Frydel, M. B. Sander, X. Huang and J. Li, *Inorg. Chem.*, 2001, **40**, 1271; (*f*) R. Horikoshi, T. Mochida, N. Maki, S. Yamada and H. Moriyama, *J. Chem. Soc., Dalton Trans.*, 2002, 28; (*g*) M. Du, X.-H. Bu, Z. Huang, S.-T. Chen, Y.-M. Guo, C. Diaz and J. Ribas, *Inorg. Chem.*, 2003, **42**, 552; (*h*) G. Férey, *Chem. Soc. Rev.*, 2008, **37**, 191; (*i*) B. Moulton and M. J. Zaworotko, *Chem. Rev.*, 2001, **101**, 1629; (*j*) H.-C. Fang, J.-Q. Zhu, L.-J. Zhou, H.-Y. Jia, S.-S. Li, X. Gong, S.-B. Li, Y.-P. Cai, P. K. Thallapally and G. J. Exarhos, *Cryst. Growth Des.*, 2010, **10**, 3277.

4 (*a*) I. Göttker-Schnetmann, D. M. Heinekey and M. Brookhart, *J. Am. Chem. Soc.*, 2006, **128**, 17114; (*b*) V. K. Praveen, S. J. George, R. Varghese, C. Vijayakumar and A. Ajayaghosh, *J. Am. Chem. Soc.*, 2006, **128**, 7542; (*c*) M. Koutmos and D. Coucouvanis, *Inorg. Chem.*, 2006, **45**, 1421; (*d*) F. Neve, A. Crispini, S. Serroni, F. Loiseau and S. Campagna, *Inorg. Chem.*, 2001, **40**, 1093; (*e*) F. F. B. J. Janssen, L. P. J. Veraart, J. M. M. Smits, R. Gelder and A. E. Rowan, *Cryst. Growth Des.*, 2011, **11**, 4313; (*f*) S. K. Dey and G. Das, *Cryst. Growth Des.*, 2011, **11**, 4463; (*g*) A. C. Wibowo, M. D. Smith and H.-C. zur Loye, *Cryst. Growth Des.*, 2011, **11**, 4449.

5 J.-W. Cui, R.-J. Zhang, Z.-G. Lin, L. Li and W.-R. Jin, *Dalton Trans.*, 2008, 895.

6 (*a*) H. Glas, K. Köhler, E. Herdtweck, P. Maas, M. Spiegler and W. R. Thiel, *Eur. J. Inorg. Chem.*, 2001, 2075; (*b*) X.-J. Zhang, C.-P. Zhao, J.-Y. Lv, C. Dong, X.-M. Ou, X.-H. Zhang and S.-T. Lee, *Cryst. Growth Des.*, 2011, **11**, 3677; (*c*) Y.-P. Cai, X.-X. Zhou, Z.-Y. Zhou, S.-Z. Zhu, P. K. Thallapally and J. Liu, *Inorg. Chem.*, 2009, **48**, 6341; (*d*) Y.-P. Cai, Q.-Y. Yu, Z.-Y. Zhou, Z.-J. Hu, H.-C. Fang, N. Wang, Q.-G. Zhan, L. Chen and Y.-P. Cai, *CrystEngComm*, 2009, **11**, 1006; (*e*) Z.-G. Gu, Y.-P. Cai, H.-C. Fang, Z.-Y. Zhou, P. K. Thallapally, J. Tian, J. Liu and G. J. Exarhos, *Chem. Commun.*, 2010, **46**, 5373.

7 (*a*) R. Cao, D.-F. Sun, Y.-C. Liang, M.-C. Hong, K. Tatsumi and Q. Shi, *Inorg. Chem.*, 2002, **41**, 2087; (*b*) M.-S. Liu, Q.-Y. Yu, Y.-P. Cai, C.-Y. Su, X.-M. Lin, X.-X. Zhou and J.-W. Cai, *Cryst. Growth Des.*, 2008, **8**, 4083; (*c*) B. Zhao, X. Y. Chen, P. Cheng, D. Z. Liao, S. P. Yan and Z. H. Jiang, *J. Am. Chem. Soc.*, 2004, **126**, 15394; (*d*) B. Zhao, H. L. Gao, X. Y. Chen, P. Cheng, W. Shi, D. Z. Liao, S. P. Yan and

Z. H. Jiang, *Chem.–Eur. J.*, 2006, **12**, 149; (*e*) X.-M. Lin, Y. Ying, L. Chen, H.-C. Fang, Z.-Y. Zhou, Q.-G. Zhan and Y.-P. Cai, *Inorg. Chem. Commun.*, 2009, **12**, 316; (*f*) X.-M. Lin, L. Chen, H.-C. Fang, Z.-Y. Zhou, X.-X. Zhou, J.-Q. Chen, A.-W. Xu and Y.-P. Cai, *Inorg. Chim. Acta*, 2009, **362**, 2619.

8 (*a*) Y.-P. Cai, G.-B. Li, Q.-G. Zhan, F. Sun, J.-G. Zhang, S. Gao and A.-W. Xu, *J. Solid State Chem.*, 2005, **178**, 3729; (*b*) Y.-P. Cai, C.-Y. Su, G.-B. Li, Z.-W. Mao, C. Zhang, A.-W. Xu and B.-S. Kang, *Inorg. Chim. Acta*, 2005, **358**, 1298; (*c*) S. K. Ghosh and P. K. Bharadwaj, *Inorg. Chem.*, 2004, **43**, 2293; (*d*) B. Zhao, L. Yi, Y. Dai, X.-Y. Chen, P. Cheng, D.-Z. Liao, S.-P. Yan and Z.-H. Jiang, *Inorg. Chem.*, 2005, **44**, 911; (*e*) J. Limburg, G. W. Brudvig and R. H. Crabtree, *J. Am. Chem. Soc.*, 1997, **119**, 2761; (*f*) X.-F. Guo, M.-L. Feng, Z.-L. Xie, J.-R. Li and X.-Y. Huang, *Dalton Trans.*, 2008, 3101; (*g*) J.-Y. Kim, A. Norquist and D. O'Hare, *J. Am. Chem. Soc.*, 2003, **125**, 12888; (*h*) X.-M. Zhang, Y.-Z. Zheng, C.-R. Li, W.-X. Zhang and X.-M. Chen, *Cryst. Growth Des.*, 2007, **7**, 980; (*i*) M.-L. Tong, S. Kitagawa, H.-C. Chang and M. Ohba, *Chem. Commun.*, 2004, 418; (*j*) X.-J. Gu and D.-F. Xue, *CrystEngComm*, 2007, **9**, 471.

9 G. M. Sheldrick, *SADABS, Version 2.05*, University of Göttingen, Göttingen, Germany.

10 G. M. Sheldrick, *SHELXS-97, Program for X-ray Crystal Structure Determination*, University of Göttingen, Göttingen, Germany, 1997.

11 G. M. Sheldrick, *SHELXS-97, Program for X-ray Crystal Structure Refinement*, University of Göttingen, Göttingen, Germany, 1997.

12 K. Nakamoto, *Infrared and Raman Spectra of Inorganic and Coordination Compounds*, John Wiley and Sons, New York, 1997.

13 (*a*) G. Wu, X.-F. Wang, T. Okamura, W.-Y. Sun and N. Ueyama, *Inorg. Chem.*, 2006, **45**, 8523; (*b*) D. M. Ciurtin, N. G. Pschirer, M. D. Smith, U. H. F. Bunz and H. C. zur Loye, *Chem. Mater.*, 2001, **13**, 2743; (*c*) Y.-B. Dong, P. Wang, R.-Q. Huang and M. D. Smith, *Inorg. Chem.*, 2004, **43**, 4727.